Photocurrent enhancement in In0.53Ga0.47As solar cells grown on InP/SiO2/Si transferred epitaxial templates

James M. Zahler, Katsuaki Tanabe, Corinne Ladous, Tom Pinnington, Frederick D. Newman, et al.

James M. Zahler, Katsuaki Tanabe, Corinne Ladous, Tom Pinnington, Frederick D. Newman, Harry A. Atwater, "Photocurrent enhancement in In0.53Ga0.47As solar cells grown on InP/SiO2/Si transferred epitaxial templates," Proc. SPIE 6649, High and Low Concentration for Solar Electric Applications II, 664909 (11 September 2007); doi: 10.1117/12.734801

Event: Solar Energy + Applications, 2007, San Diego, California, United States

Photocurrent Enhancement in $In_{0.53}Ga_{0.47}As$ Solar Cells Grown on $InP/SiO_2/Si$ Transferred Epitaxial Templates

James M. Zahler[a], Katsuaki Tanabe*[b], Corinne Ladous[a], Tom Pinnington[a],
Frederick D. Newman[c], Harry A. Atwater[b]
[a]Aonex Technologies, Pasadena, CA 91106, USA,
[b]Thomas J. Watson Laboratory of Applied Physics, California Institute of Technology, Pasadena, CA 91125, USA,
[c]Emcore Photovoltaics, Albuquerque, NM 87123, USA

ABSTRACT

InP/Si engineered substrates formed by wafer bonding and layer transfer have the potential to significantly reduce the cost and weight of III-V compound semiconductor solar cells. InP/Si substrates were prepared by He implantation of InP prior to bonding to a thermally oxidized Si substrate and annealing to exfoliate an InP thin film. Following thinning of the transferred InP film to remove surface damage caused by the implantation and exfoliation process, InGaAs solar cells lattice-matched to bulk InP were grown on these substrates using metal-organic chemical vapor deposition. The photovoltaic current-voltage characteristics of the InGaAs cells fabricated on the wafer-bonded InP/Si substrates were comparable to those synthesized on commercially available epi-ready InP substrates, and had a ~20% higher short-circuit current which we attribute to the high reflectivity of the $InP/SiO_2/Si$ bonding interface. This work provides an initial demonstration of wafer-bonded InP/Si substrates as an alternative to bulk InP substrates for solar cell applications.

Keywords: solar cells, wafer bonding, layer transfer, III-V, InGaAs, InP, Si, SiO_2, low cost, epitaxial growth

1. INTRODUCTION

Engineered substrates consisting of thin films of InP on Si handle substrates (InP/Si substrates or epitaxial templates) have the potential to significantly reduce the cost and weight of compound semiconductor solar cells relative to those fabricated on bulk InP substrates. InGaAs solar cells on InP have superior performance to Ge cells at photon energies greater than 0.7 eV. The current record efficiency cell for 1 sun illumination was achieved using an InGaP/GaAs/InGaAs triple junction cell design with an InGaAs bottom cell [1]. Thermophotovoltaic (TPV) cells from the InGaAsP-family of III-V materials grown epitaxially on InP substrates would also benefit from such an InP/Si substrate [2]. Additionally, a proposed four-junction solar cell fabricated by joining subcells of InGaAs and InGaAsP grown on InP with subcells of GaAs and AlInGaP grown on GaAs through a wafer-bonded interconnect would enable the independent selection of the subcell band gaps from well developed materials grown on lattice matched substrates [3,4] (Figure 1). Substitution of InP/Si substrates for bulk InP in the fabrication of such a four-junction solar cell could significantly reduce the substrate cost as described below.

Direct heteroepitaxial growth of InP thin films on Si substrates has not produced the low dislocation-density high quality layers required for active InGaAs/InP in optoelectronic devices due to the ~8% lattice mismatch between InP and Si [5]. Wafer bonding on the other hand is not subject to lattice matching limitations associated with epitaxial growth, and has been used to fabricate materials that consist of crystalline semiconductors on amorphous materials and also to integrate crystalline materials of different lattice constants. For the integration of both crystalline-amorphous and crystalline-crystalline pairs, defects caused by the lack of crystallographic registry are isolated to the wafer-bonded interface. Thus, provided the wafer-bonded interface does not play an active role in the operation of the device, the independent materials and devices fabricated in them can in principle have performance typical of devices made on or in the bulk material.

*tanabe@caltech.edu; phone 1 626 395-2193; fax 1 626 844-9320; daedalus.caltech.edu

High and Low Concentration for Solar Electric Applications II, edited by Martha Symko-Davies,
Proc. of SPIE Vol. 6649, 664909, (2007) · 0277-786X/07/$18 · doi: 10.1117/12.734801

Layer transfer of a high quality single crystal InP film onto a Si bulk substrate can be accomplished through wafer bonding of InP to Si and exfoliation of a thin film from the InP wafer induced by implantation of light elements such as hydrogen and helium [6-8]. The implantation process results in a high density of point defects near the region where exfoliation occurs, however most of this region can be removed by thinning the transferred film. Furthermore, the point defects generated by the implantation process have previously been shown to have minimal impact on the quality of InP grown on transferred thin films of InP [9]. This is likely because during the epitaxial process, vacancies in the growth surface are occupied by the appropriate anion or cation adatom. Because only a few μm of InP are consumed in the transfer of a film and subsequent reclaim of the InP substrate, a single InP wafer could be reused repeatedly to generate many InP/Si substrates, thus reducing the material cost of InP in devices grown on those substrates. In this paper, we describe the fabrication of wafer-bonded InP/Si substrates and report results from the first known demonstration of InGaAs solar cell fabrication on InP/Si epitaxial engineered substrates.

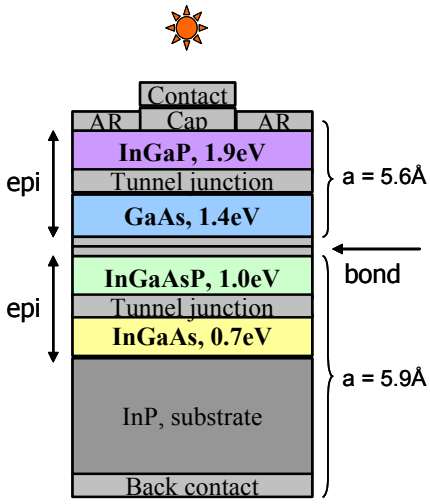

Fig. 1. Cross-sectional schematic of the bonded (Al)InGaP/GaAs/InGaAsP/InGaAs four-junction solar cell.

2. EXPERIMENTAL

InP (001) substrates and thermally oxidized Si (001) handle substrates were used for the fabrication of InP/Si substrates for growth of InGaAs solar cell test structures. However, experiments were also conducted with Si (001) substrates that had been coated with a silicon dioxide (SiO_2) film using plasma-enhanced chemical vapor deposition (PECVD) from a tetraethyl orthosilicate (TEOS) precursor. The PECVD oxide was subsequently densified by annealing and subjected to a chemical mechanical polish (CMP) to give a particle-free smooth bonding surface. Use of a SiO_2 film was found to improve the thermal stability of the bonded interface relative to structures fabricated with a direct semiconductor-semiconductor bond. InP/Si substrates fabricated with handle substrates having thermal or CVD-deposited oxides resulted in >90% layer transfer and good subsequent thermal stability. The first step in the InP/Si substrate fabrication was the ion implantation of the InP wafer with He^+ at an energy between 115 and 180 keV to a dose of at least $1.0x10^{17}$ cm^{-2}. Prior to wafer bonding the surfaces of both the InP and the Si handle substrates were prepared by wet chemical cleaning to remove organic and particulate contamination followed by activation of the bonding surfaces with an atmospheric pressure plasma exposure. Bonding between the InP and the Si handle was then initiated at a temperature of 150 ^oC or greater. The two substrates were then annealed under uniaxial pressure greater than 1 MPa to promote the formation of covalent bonds between the InP and Si substrates and induce the exfoliation of a thin layer (~900 nm) of InP thus forming the InP/Si substrate.

The film was transferred from an InP substrate implanted with He^+ to a dose of $1.0x10^{17}$ cm^{-2} at an energy of 180 keV. The transferred InP film thickness was ~900 nm. In excess of 90% of the film area was transferred with minimal macroscopic defects in the as-transferred film.

To test the performance of III-V compound active photovoltaic device layers grown on the wafer-bonded InP/Si substrates in functional solar cell structures, single-junction InGaAs solar cells were grown on both InP/Si substrates and commercial bulk epi-ready InP (001) substrates as a reference by metal-organic chemical vapor deposition (MOCVD). Each of the solar cells had an n-type $In_{0.53}Ga_{0.47}As$ emitter and a p-type $In_{0.53}Ga_{0.47}As$ base with bandgap energy of 0.74 eV, nominally lattice-matched to (001) InP. Although we have not investigated the strain in these epitaxial InGaAs layers in detail yet, it is supposed that they are under tensile strain due to the difference in thermal expansion between InP and Si from the analysis with a similar heterostructure in Reference 7. The cells were designed to enable convenient and low-resistance contact to both base and emitter through the top surface of the cell. A schematic of the InGaAs cell structure is shown in Figure 2. The cell growth begins with a 1 μm thick InP buffer layer doped n-type with a target carrier concentration of $1x10^{19}$ cm^{-3} that functions as a current spreading layer for lateral back side contact. Back side and front side contacts were made using Ti/Au contacts on n-type InGaAs doped with a target carrier concentration of $1x10^{19}$ cm^{-3}. Typical optical micrographs of the front contact pads and grids of the InGaAs solar cells grown on the InP/Si substrates and on bulk InP (001) substrates are shown in Figure 3. An InGaAs tunnel-junction was used to switch the carrier type from the p-type in the base to n-type in the back side contact structure, allowing the front and back contacts to be fabricated with a single lithographic process. The remainder of the structure was typical of a single-junction InGaAs cell consisting of an InP window layer, a 300 nm thick n-type InGaAs emitter doped with a carrier concentration of $5x10^{18}$ cm^{-3}, a 3 μm thick p-type InGaAs base doped with a carrier concentration of $1x10^{17}$ cm^{-3}, and a 50 nm thick p-type InP back side field layer doped with a carrier concentration of $1\text{-}2x10^{18}$ cm^{-3}. No anti-reflective coating was used in the fabrication of the test cells.

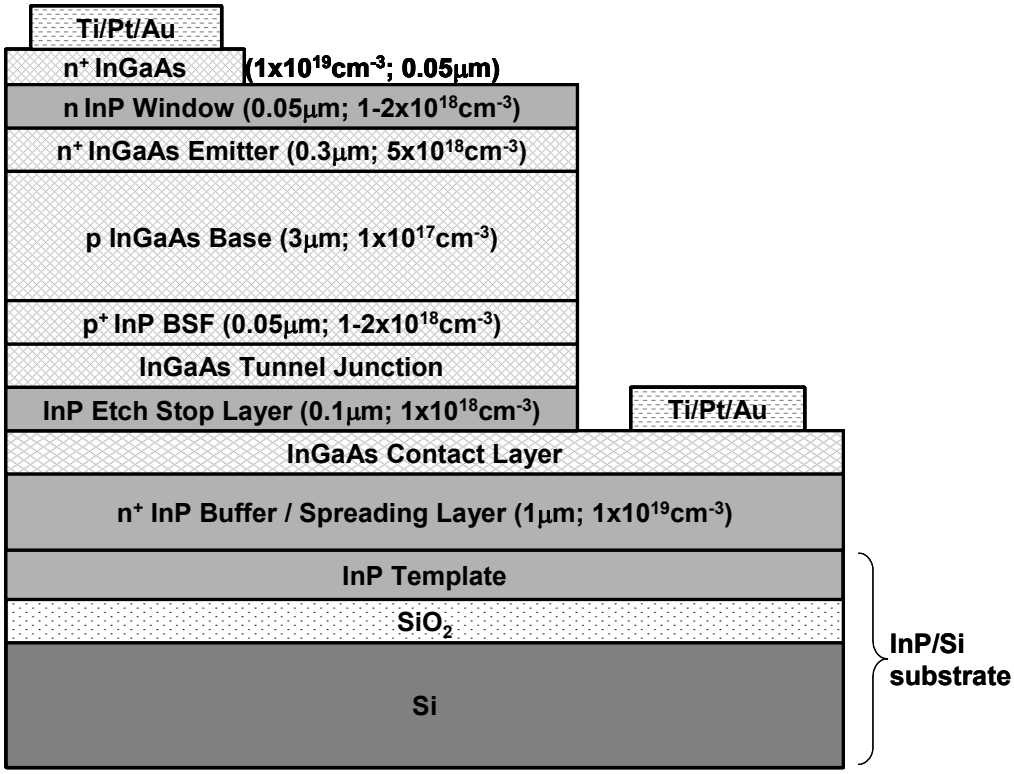

Fig. 2. Schematic cross-sectional view of the InGaAs solar cell grown on the InP/Si substrates.

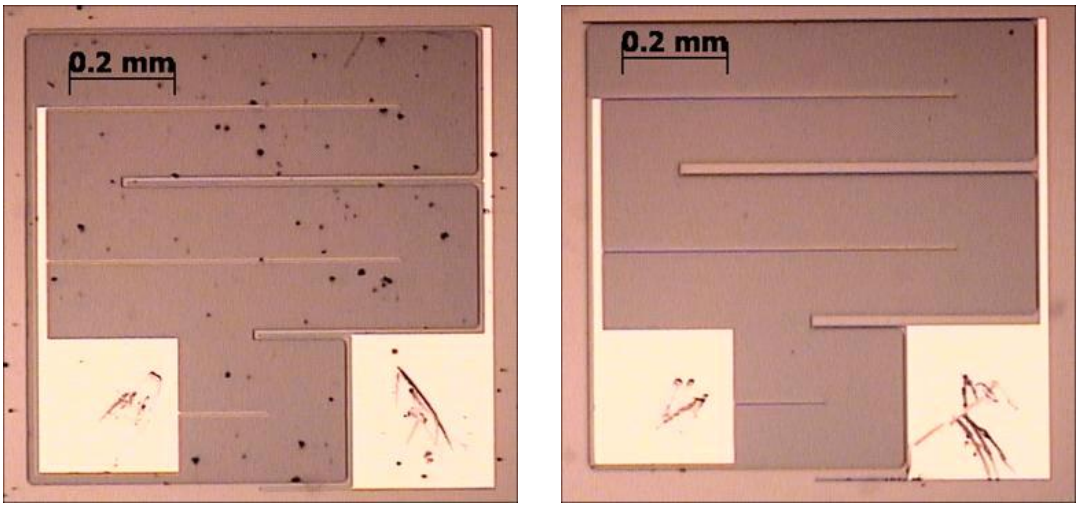

Fig. 3. Optical micrographs of the InGaAs cells, including contact pads and grids, fabricated on (left) an InP/Si substrate and (right) a bulk InP (001) substrate. The contact pad on the left is the n-side contact and the pad on the right is the p-side contact.

3. RESULTS AND DISCUSSION

The ion implantation induced exfoliation process results in lattice damage in the transferred film with a damage peak roughly coinciding with region where exfoliation occurs. Thus, in the as-transferred InP/Si structure there is a distribution of lattice defects with a peak at the surface of the transferred film decreasing to a minimum defect density in the material adjacent to the bonded interface. We observed cross-sectional transmission electron microscopy (XTEM) of a film transferred from InP implanted with 115 keV He^+ to a dose of $1.0x10^{17}$ cm^{-2} and its selected area diffraction (SAD) pattern showed that the InP adjacent to the bonded interface is single-crystalline. Close inspection of the defect structure using high-resolution XTEM imaging showed that the strain contrast is caused by a both extended defects that can be directly imaged and point defects such as vacancies and interstitials. It is essential that the damage in the as-transferred InP thin film in InP/Si engineered substrates be minimized prior to epitaxial growth of III-V materials. In particular, extended defects that intersect the growth surface are problematic for growth. For the InP/Si substrates used for growth of InGaAs test cells, the damaged surface region of the as-transferred InP film was removed leaving a film of ~400 nm thickness. The transferred films were thinned using a combination of inductively-coupled plasma reactive ion etching (ICP-RIE) for damage removal and a wet chemical etch for surface smoothing. Contact-mode atomic force microscopy (AFM) measurements of the InP/Si substrates showed that the as-transferred roughness of >10 nm-rms was reduced to 5-10 nm-rms following the etching process. More importantly, the most heavily damaged material at the surface of the InP transferred layer was removed.

Light current-voltage (I-V) characteristics of the InGaAs cells grown on the InP/Si substrates and on bulk InP (001) substrates were measured under AM1.5 Global illumination truncated at 850 nm by a long-pass filter, to mimic the optical configuration of subcells under a GaAs cell. The resulting I-V data are shown in Figure 4. The device parameters for the InGaAs cell grown on the wafer-bonded InP/Si substrate were J_{sc} = 24.9 mA cm^{-2}, V_{oc} = 0.30 V and FF = 0.66, where J_{sc}, V_{oc} and FF are short-circuit current, open-circuit voltage and fill factor, respectively. This performance was comparable to that of the InGaAs cells grown on bulk InP (001) substrates, J_{sc} = 21.5 mA cm^{-2}, V_{oc} = 0.31 V and FF = 0.70. Figure 5 shows the spectral responses for the InGaAs solar cells grown on the InP/Si substrate and a bulk InP substrate.

The larger J_{sc} and the higher quantum efficiency for the cell grown on the InP/Si substrate are attributed to enhanced light trapping effects in the wafer-bonded cell structure, due primarily to reflection at the bonding interfaces. Noting the large refractive index difference at the InP/SiO_2/Si bonding interface, $n_{InP} \sim 3.5$, $n_{SiO2} \sim 1.5$ and $n_{Si} \sim 3.5$ in the IR region, the reflectivity at the InP/SiO_2/Si interface was estimated as follows [10].

$$R_{tot} = \left| \frac{r_1 + r_2 e^{-2i\delta}}{1 + r_1 r_2 e^{-2i\delta}} \right|^2 , \quad (1)$$

where

$$r_j = \frac{N_{j-1} - N_j}{N_{j-1} + N_j} \quad (2)$$

and

$$\delta = \frac{2\pi}{\lambda} n_1 d_1 . \quad (3)$$

The subscript j denotes the layer, where the InP, SiO_2 and Si layers correspond to j = 0, 1 and 2, respectively. Note that the refractive indices N_j are generally complex functions of wavelength and are expressed as $N_j = n_j + ik_j$, where both n_j and k_j are real. λ is the wavelength in vacuum and the thickness of the SiO_2 layer, d_1, was set to 420 nm as determined by ellipsometry measurement. For the optical constants of $In_{0.53}Ga_{0.47}As$, the data in Reference 11 was used with a modification of the imaginary part of the dielectric constant, ε_2, fit to the power law around at the absorption edge [12],

$$\varepsilon_2(\omega) \propto \frac{(\hbar\omega - E_g)^{1/2}}{(\hbar\omega)^2} . \quad (4)$$

The bandgap energy E_g of $In_{0.53}Ga_{0.47}As$ was set to be 0.73 eV. The optical constants of Si, SiO_2 and InP were adopted from Reference 13. The reflectivity at the $In_{0.53}Ga_{0.47}As$/InP interface was also estimated as a reference simply by determining $|r_1|$ from Equation 2, where the $In_{0.53}Ga_{0.47}As$ and InP layers correspond to j = 0 and 1, respectively. Based on this calculation the reflectivity of the InP/SiO_2/Si interface is estimated to be ~0.5 at maximum in the IR range for normal incidence due to the large refractive index differences at the InP/SiO_2 and SiO_2/Si interfaces, as shown in Figure 6. On the other hand, the reflectivity at the $In_{0.53}Ga_{0.47}As$/InP interface is negligibly small compared with that at the InP/SiO_2/Si bonding interface, as seen in Figure 6, due to the small difference in the refractive indices between $In_{0.53}Ga_{0.47}As$ and InP, $n_{In0.53Ga0.47As} \sim n_{InP} \sim 3.5$ in the IR region. Particularly the reflectivity of the InP/SiO_2/Si interface significantly increases after 1200 nm, which well explains the enhanced photocurrent for the InGaAs cell grown on the InP/Si substrate relative to that on a bulk InP substrate seen in the spectral responses of Figure 5.

Absorption in the $In_{0.53}Ga_{0.47}As$ layer was also calculated using a one-dimensional optical computational package [14]. This simulation was performed for a structure consisting of air/ $In_{0.53}Ga_{0.47}As$ (3650 nm)/ InP (1400 nm)/ SiO_2 (420 nm)/ Si for the cell on the InP/Si substrate and air/ $In_{0.53}Ga_{0.47}As$ (3650 nm)/ InP for the reference cell grown on a bulk InP substrate. The enhanced photocurrent and the oscillatory variation of the spectral quantum efficiency for the InGaAs cell on the InP/Si substrate were well-modeled by a simple one-dimensional optical calculation of the absorbance of the $In_{0.53}Ga_{0.47}As$ layer in the $In_{0.53}Ga_{0.47}As$/InP/SiO_2/Si structure relative to the $In_{0.53}Ga_{0.47}As$/InP reference structure, as shown in Figure 5.

Light trapping effects might also be enhanced by the slightly rougher top surface for cells grown on InP/Si substrates, attributable to the increased roughness of the InP/Si substrate growth surface (~10 nm-rms), relative to the bulk, epi-ready InP (001) substrates (<1 nm-rms) [15,16]. This light I-V characteristic result indicates that the fabricated InP/Si substrates are promising alternative substrates to InP bulk wafers for InGaAs solar cell fabrication. The obtained J_{sc} of 24.9 mA cm^{-2} for the InGaAs cell on the InP/Si substrate is large enough to current match to state-of-art InGaP/GaAs two-junction cells [17,18]. This InGaAs cell is therefore a strong candidate for the bottom cell of an ultrahigh efficiency three-junction cell with its significantly higher V_{oc} than the conventional Ge bottom cell [19-21].

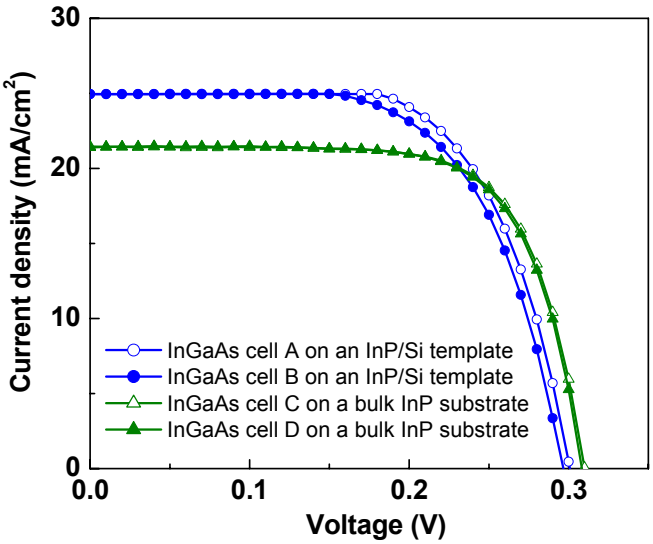

Fig. 4. Typical light I-V curves for the $In_{0.53}Ga_{0.47}As$ solar cells grown on an InP/Si substrate and on a commercial epi-ready InP substrate. The I-V measurements were performed under AM1.5G illumination truncated at 850 nm.

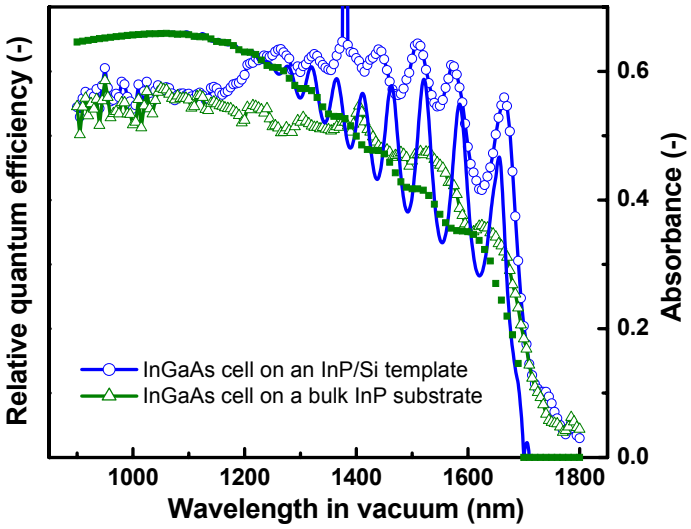

Fig. 5. Measured spectral responses for the $In_{0.53}Ga_{0.47}As$ solar cells grown on an InP/Si substrate and on a commercial epi-ready InP substrate. The calculated absorbance of the $In_{0.53}Ga_{0.47}As$ layer for $In_{0.53}Ga_{0.47}As/InP/SiO_2/Si$ (solid line) and $In_{0.53}Ga_{0.47}As/InP$ (dot line) structures are also plotted.

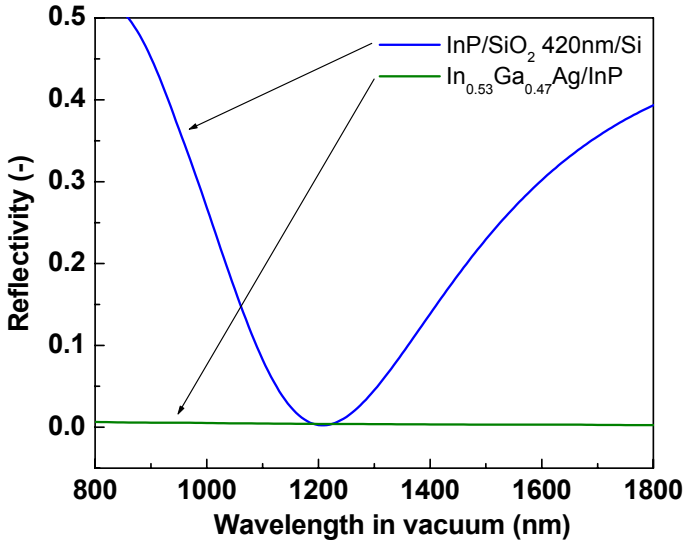

Fig. 6. Calculated reflectivities of the $InP/SiO_2/Si$ and $In_{0.53}Ga_{0.47}As/InP$ interfaces.

4. CONCLUSIONS

We have demonstrated InGaAs solar cell fabrication on layer-transferred InP/Si substrates. Such InP/Si substrates could be used as substrates for InGaAsP/InGaAs dual-junction solar cells lattice-matched to InP as well as conventional InP single-junction cells. Ultimately, InP/Si substrates are extendable to fabrication of ultrahigh efficiency four-junction AlInGaP/GaAs/InGaAsP/InGaAs cells via a direct bond interconnect between subcell structures of InGaAsP/InGaAs grown on InP/Si and AlInGaP/GaAs grown on GaAs to form the overall four junction cell structure.

ACKNOWLEDGEMENTS

The authors would like to thank Anna Fontcuberta i Morral of the Walter Schottky Institute for her work in the development of the InP/Si substrate fabrication process. The work at Aonex Technologies was supported by a Small Business Innovation Research (SBIR) awarded and administered by the Air Force Research Laboratory (AFRL). The Caltech portion of this work was supported by the National Renewable Energy Laboratory (NREL) subcontract no. XAT-4-33624-10.

REFERENCES

1. J. F. Geisz, S. R. Kurtz, M. W. Wanlass, J. S. Ward, A. Duda, D. J. Friedman, J. M. Olson, W. E. McMahon, T. E. Moriarty, and J. T. Kiehl, *Appl. Phys. Lett.* **91**, 023502 (2007).
2. M. W. Wanlass, J. S. Ward, K. A. Emery, M. M. Al-Jassim, K. M. Jones, and T. J. Coutts, *Sol. Ener. Sol. Cell.* **41**, 405 (1996).
3. J. M. Zahler, A. Fontcuberta i Morral, C. G. Ahn, H. A. Atwater, M. W. Wanlass, C. Chu, and P. A. Iles, *Proceedings of the 29th IEEE Photovoltaic Specialists Conference* (IEEE, New York, 2002), p. 45.

4. K. Tanabe, D. J. Aiken, M. W. Wanlass, A. Fontcuberta i Morral, and H. A. Atwater, *Appl. Phys. Lett.* **89**, 102106 (2006).
5. M. Sugo, Y. Takanashi, M. M. Al-Jassim, and M. Yamaguchi, *J. Appl. Phys.* **68**, 540 (1990).
6. Q. Y. Tong, Y. L. Chao, L. J. Huang, and U. Gosele, *Electron. Lett.* **35**, 341 (1999).
7. A. Fontcuberta i Morral, J. M. Zahler, S. P. Ahrenkiel, M. W. Wanlass, and H. A. Atwater, *Appl. Phys. Lett.* **83**, 5413 (2003).
8. A. Fontcuberta i Morral, J. M. Zahler, M. J. Griggs, H. A. Atwater, and Y. J. Chabal, *Phys. Rev. B* **72**, 085219 (2005).
9. S. Hayashi, R. Sandhu, M. Wojtowicz, G. Chen, R. Hicks, M. S. Goorsky, *J. Appl. Phys.* **98**, 093526 (2005).
10. O. S. Heavens, *Optical Properties of Thin Solid Films*, Butterworths Scientific Publications, London, 1955.
11. M. A. Afromowitz, *Solid State Comm.* **15**, 59-63 (1974).
12. S. Adachi, *J. Appl. Phys.* **66** (12), 6030-6040 (1989).
13. E. D. Palik, ed., *Handbook of Optical Constants of Solids*, Academic Press, Orland, 1985.
14. SpectraRay II, SENTECH Instruments GmbH, 2006.
15. E. Yablonovitch and G. D. Cody, *IEEE Trans. Electron. Devices* **ED-29**, 300 (1982).
16. J. H. Hu and R. G. Gordon, *Solar Cells* **30**, 437 (1991).
17. T. Takamoto, E. Ikeda, H. Kurita, and M. Ohmori, *Appl. Phys. Lett.* **70**, 381 (1997).
18. D. B. Jackrel, S. R. Bank, H. B. Yuen, M. A. Wistey, J. S. Harris, A. J. Ptak, S. W. Johnson, D. J. Friedman, S. R. Kurtz, *J. Appl. Phys.* **101**, 114916 (2007).
19. D. J. Friedman and J. M. Olson, *Prog. Photovolt.* **9**, 179 (2001).
20. J. M. Olson, D. J. Friedman, and S. R. Kurtz, in *Handbook of Photovoltaic Science and Engineering*, edited by A. Luque and S. Hegedus (Wiley, New York, 2003), p. 359.
21. R. R. King, R. A. Sherif, G. S. Kinsey, S. R. Kurtz, C. M. Fetzer, K. M. Edmondson, D. C. Law, H. L. Cotal, D. D. Krut, J. H. Ermer, and N. H. Karam, *Proceedings of the International Conference on Solar Concentrators for the Generation of Electricity or Hydrogen* (NREL, Golden, 2005).